Synthetic and Systems Biotechnology 9 (2024) 694–700

Contents lists available at ScienceDirect

Synthetic and Systems Biotechnology

journal homepage: www.keaipublishing.com/en/journals/synthetic-and-systems-biotechnology

Original Research Article

Biochemical synthesis of taxanes from mevalonate

Jing Li [a,b,c,1], Xiaonan Liu [a,c,d,1,***], Xiaoxi Zhu [a,c,d,1], Jiayu Liu [a,c], Lei Zhang [a,c], Nida Ahmed [a,c,d], Jian Qi [a,c,d], Bihuan Chen [a,c], Daliang Tang [e], Jinsheng Yu [e], Zhijin Fan [b,d,**], Huifeng Jiang [a,c,*]

[a] Key Laboratory of Engineering Biology for Low-carbon Manufacturing, Tianjin Institute of Industrial Biotechnology, Chinese Academy of Sciences, Tianjin, 300308, China
[b] State Key Laboratory of Elemento-Organic Chemistry, College of Chemistry, Nankai University, Tianjin, 300071, China
[c] National Center of Technology Innovation for Synthetic Biology, Tianjin, 300308, China
[d] University of Chinese Academy of Sciences, Beijing, 100049, China
[e] Shanghai Engineering Research Center of Molecular Therapeutics and New Drug Development, School of Chemistry and Molecular Engineering, East China Normal University, Shanghai, 200062, China

ARTICLE INFO

Keywords:
Biochemical synthesis
Taxanes
Paclitaxel
Modular synthesis

ABSTRACT

Taxanes are kinds of diterpenoids with important bioactivities, such as paclitaxel (taxol®) is an excellent natural broad-spectrum anticancer drug. Attempts to biosynthesize taxanes have made with limited success, mainly due to the bottleneck of the low efficiency catalytic elements. In this study, we developed an artificial synthetic system to produce taxanes from mevalonate (MVA) by coupling biological and chemical methods, which comprises *in vitro* multi-enzyme catalytic module, chemical catalytic module and yeast cell catalytic module. Through optimizing *in vitro* multienzyme catalytic system, the yield of taxadiene was increased to 946.7 mg/L from MVA within 8 h and the productivity was 14.2-fold higher than microbial fermentation. By incorporating palladium catalysis, the conversion rate of Taxa-4(20),11(12)-dien-5α-yl acetate (T5α-AC) reached 48 %, effectively addressing the product promiscuity and the low yield rate of T5αOH. Finally, we optimized the expression of T10βOH in yeast resulting in the biosynthesis of Taxa-4(20),11(12)-dien-5α-acetoxy-10β-ol(T5α-AC-10β-ol) at a production of 15.8 mg/L, which displayed more than 2000-fold higher than that produced by co-culture fermentation strategy. These technologies offered a promising new approach for efficient synthesis of taxanes.

1. Introduction

Taxanes are a class of tetracyclic diterpenoids with high-value pharmacological activity, which include paclitaxel, docetaxel, cabazitaxel, and various taxane skeleton derivatives. Paclitaxel (taxol®) as a famous anticancer drug is mainly extracted from the bark of endangered *Taxus* [1] and has attracted significant interests due to its excellent anti-cancer properties, complex synthesis process and limited yield [2]. With decades of persistent efforts, the catalytic elements involved in the biosynthetic pathway of paclitaxel have been fully elucidated [3–5], especially for the recent works on oxetane ring formation has facilitated the acquisition of a minimum gene set for baccatin III biosynthesis [3,4]. However, researches on the specific catalytic reaction sequences and the heterologous synthesis abilities of paclitaxel have been limited since the first discovery in the 1960s [5,6].

The promiscuity and low catalytic efficiency of the first P450 enzyme taxadiene-5α-hydroxylase (T5αOH) remain a major bottleneck and the deficiency of intermediates thus leads to more difficulties in elucidating the subsequent catalytic process of unknown P450 enzymes [7,8]. Scientists have reported that T5αOH catalyzes taxadiene to a kind of

Peer review under responsibility of KeAi Communications Co., Ltd.
* Corresponding author. Key Laboratory of Engineering Biology for Low-carbon Manufacturing, Tianjin Institute of Industrial Biotechnology, Chinese Academy of Sciences, Tianjin, 300308, China.
** Corresponding author. State Key Laboratory of Elemento-Organic Chemistry, College of Chemistry, Nankai University, Tianjin, 300071, China.
*** Key Laboratory of Engineering Biology for Low-carbon Manufacturing, Tianjin Institute of Industrial Biotechnology, Chinese Academy of Sciences, Tianjin, 300308, China
E-mail addresses: liu_xn@tib.cas.cn (X. Liu), fanzj@nankai.edu.cn (Z. Fan), jiang_hf@tib.cas.cn (H. Jiang).
[1] These authors contributed equally to this article: Jing Li, Xiaonan Liu and Xiaoxi Zhu.

https://doi.org/10.1016/j.synbio.2024.05.002
Received 8 February 2024; Received in revised form 22 April 2024; Accepted 6 May 2024
Available online 13 May 2024

epoxide intermediate that spontaneously rearranged mainly to iso-OCT and OCT rather than target product taxadiene-5α-ol [7,9]. Moreover, when T5αOH is expressed in tobacco, the number of oxidation products of taxadiene reaches as many as 36 kinds [6]. Directed mutagenesis and expression optimization were carried out with continuous efforts, but were unable to improve the oxidation selectivity effectively [1,6,8,10]. Studies reveal that taxadien-5α-ol acetyltransferase (TAT) is a multi-specific enzyme and the by-product of geranylgeraniol (GGOH) can also be acetylized by TAT, which could lead to a distribution of the acetylation precursors [5,11]. Therefore, we expected to refer a biochemical catalytic method to synthesize paclitaxel intermediates by circumventing these two-step reactions.

Since the first total chemical synthesis route was achieved in 1994, paclitaxel has been one of the most popular target molecules in the field of organic synthetic chemistry, and eleven total synthesis methods have been reported until now [12]. It is worth mentioning that Li et al. [13] created a 21-step asymmetric total synthesis route using a samarium diiodide-mediated pinacol coupling reaction, which is currently the shortest total synthesis route for paclitaxel, but the overall yield is only 0.118 %. Thus, severe challenges still existed in chemical synthesis, including the redundant pathways and low reaction yields. Therefore, it is imperative to synthesize taxanes by leveraging the advantages of both biocatalysis and chemical reactions.

The upstream biosynthetic route of taxanes starts from the mevalonate (MVA) pathway or methylerythritol phosphate (MEP) pathway. Compared with the MEP pathway, the MVA pathway is currently a research focus in metabolic engineering for the synthesis of terpenoid compounds, due to its advantages such as higher efficiency, better controllability, and lower requirement for cofactors. The cell-free system has been expropriated to produce the amorphadiene [14] and farnesene [15], this production mode avoids complex host cell metabolic engineering, cytotoxicity of intermediates and endogenous competition pathways [16]. In addition, an isopentenol utilization pathway (IUP) was established to produce taxadiene *in vitro*. However, due to isoprenol is not the original substrate for choline kinase (CK), high substrate concentrations needs to be added and the substrate toxicity caused enzymes to precipitate [17]. Therefore, the MVA pathway was considered for taxanes synthesis in this study. Among this pathway, the upstream CoA-derived intermediates such as Ac-CoA, acetoacetyl-CoA (AcAc--CoA) and hydroxymethylglutaryl-CoA (HMG-CoA) contain an adenosine moiety, which can be hydrolyzed extracellularly to generate phosphopeptides and adenosine diphosphate (ADP) [18]. In addition, phosphate ions are sensitive to the ionicity and polarity of the environment [19], thereby affecting the stability of downstream phosphorylated intermediates. Hence, compared to these intermediates mentioned above, MVA is more favorable as a precursor in a cell-free systems due to its stability and lower cost.

Here, we proposed a combinatorial approaches strategy for synthesizing precious taxanes involved in the synthetic pathway of paclitaxel, such as taxadiene, T5α-AC, and T5α-AC-10β-ol with combining cell-free enzymatic reaction system, chemocatalysis, and whole-cell catalysis (Fig. 1). By coupling biological and chemical reaction system and using MVA as the starting point, we successfully circumvented the bottleneck of the T5αOH and TAT steps, optimized the reaction process, and achieved efficient synthesis of the rare paclitaxel intermediate T5α-AC. Furthermore, through optimized expression of T10βOH, we successfully converted T5α-AC into T5α-AC-10β-ol. Moreover, the accumulation of T5α-AC and T5α-AC-10β-ol will facilitate future understanding and decoding of the complete biosynthetic pathway of paclitaxel.

2. Results

2.1. Establishing a cell-free synthetic system for taxadiene

Our primary focus was on establishing an *in vitro* taxadiene synthetic system using MVA as a precursor [20]. This system recruited a cascade

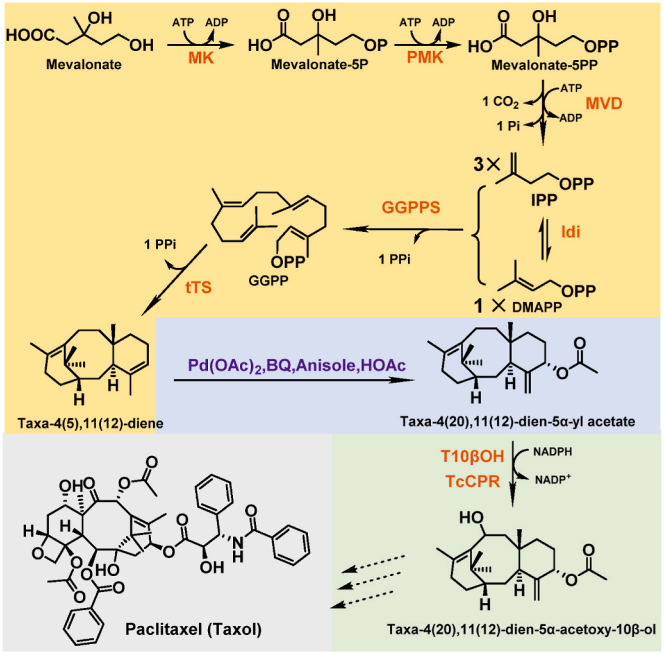

Fig. 1. The diagram of biochemical synthesis system for conversion of mevalonate (MVA) to paclitaxel. Auxiliary enzymes and chemicals are indicated. Sections in orange-yellow and green color depict enzymatic catalysis. The chemical catalysis is shown in purple.

of enzymes, including mevalonate kinase (MK), phosphomevalonate kinase (PMK), mevalonate pyrophosphate decarboxylase (MVD), isopentenyl diphosphate isomerase (IDI), GGPPS and truncated TS, to facilitate taxadiene synthesis. As shown in Fig. S1, these six enzymes were solubly expressed in *Escherichia coli*. The artificial metabolic flux from MVA to taxadiene was monitored through GC-MS analysis. The reaction systems from MVA to taxadiene were constructed in both phosphate buffer and Tris-HCl buffer, where the production of taxadiene in Tris-HCl buffer was 3.6 folds higher than that in phosphate buffer, reaching a production level of 0.22 mg/L (Fig. 2B, Figs. S2 and S4).

According to the proof-of-concept system, we proceeded to optimize it by regulating reaction factors step by step. Firstly, we focused on optimizing the reaction temperature and pH, and the results showed that 30 °C and pH 8.0 were preferred for the yield of taxadiene (Fig. 2C and Fig. S4). In addition, by monitoring the reaction time, we discovered that the maximum yield of taxadiene of 0.31 mg/L was achieved at approximately 4 h with 1 mM MVA substrate (Fig. S5). Secondly, we turned our attention to optimize the cofactors used in this system. Since the first three steps of the reaction pathway require ATP, we introduced polyphosphate kinase (PPK) with polyphosphate as a donor to regenerate ATP within the system. The results showed that the ATP cycle led to about 20 % increase in production compared to the previous system (Fig. 2C and Fig. S6). However, the visible white precipitates within the system indicated that the addition of polyphosphate had a strong inhibitory effect on enzymes [21]. Therefore, the phosphate donor was opted to pyrophosphate (PPi) instead of polyphosphate. Additionally, we replaced the initial PPK enzyme with PPK2C^{paN} from *Pseudomonas aeruginosa* [19], as it exhibited higher affinity and catalytic efficiency towards PPi. This modification resulted in more favorable condition with 1.2 mM PPi, 5 mM ATP and 10 mM Mg^{2+}, leading to a 1.7-fold increase in production (Fig. S7 and Fig. S8).

2.2. Optimization of taxadiene synthetic system

Previous studies on *in vivo* and *in vitro* biosynthesis of terpenoids have shown that there is a significant catalytic mismatch between

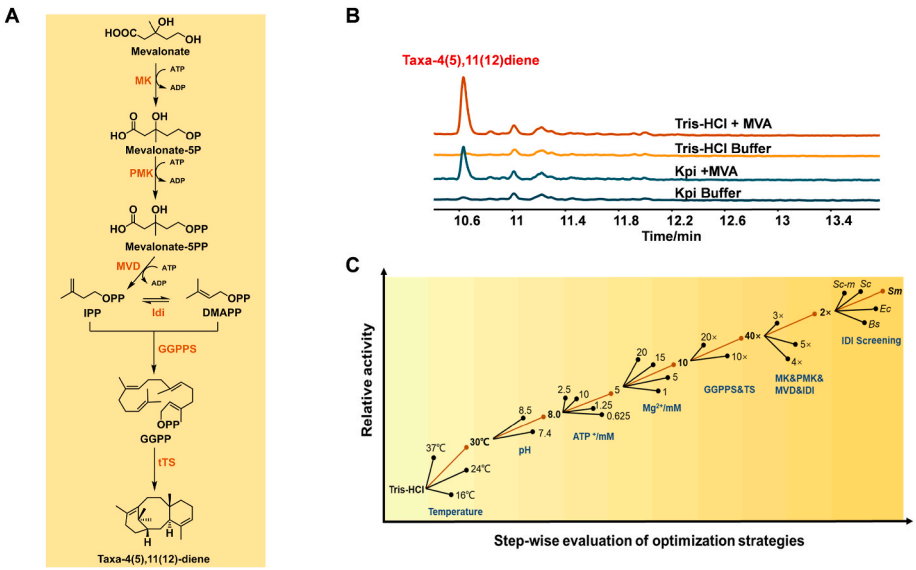

Fig. 2. Enzymatic synthesis of taxadiene from MVA.
(A) The schematic depiction of enzymatic synthesis of taxadiene from MVA.
(B) GC analysis of taxadiene from MVA *in vitro* with different buffers.
(C)*In vitro* optimization for the biosynthesis of taxadiene from 1 mM MVA. Blue indicates the optimization strategies in turn, and red indicates the optimal conditions under each strategy, which are then used to evaluate the next strategy. The Y-axis represents the relative yield of taxadiene under different conditions.

downstream terpenoid synthase module and upstream MVA pathway module [22–24]. Hence we divided taxadiene pathway into two parts for enzyme quantity optimization, including part I (MK&PMK&MVD&PPK&IDI) and part II (GGPPS&tTS) [16,25]. Based on our results, 2 × loading of the part I and 40 × loading of the part II in the system effectively resulted in production increase of 1.2 times and 5.4 times, respectively (Fig. 2C and Fig. S9). After that, the enzymatic productions flux from MVA to taxadiene were iteratively optimized so that the capability of cell-free system could be improved. As a rate-limiting enzyme for terpenoids production within the MVA pathway [15], we firstly screened IDI from six different sources to enhance the conversion of four equivalents of MVA into three equivalents of IPP and one equivalent of DMAPP. The IDI derived from *Salviae miltiorrhizae* demonstrated the highest activity, approximately twice as active as the IDI derived from *E. coli* (Fig. 3A). Next step, we engineered and expressed the fusion protein BST1-ERG20, which could facilitate the conversion of IPP and DMAPP into GGPP [26,27] by enhancing the flux of GPP and FPP to GGPP. The results indicated that the inclusion of 20 μM BST1-ERG20 led to a 27 % increase in taxadiene production (Fig. S10A). Simultaneously, on account of the instability of the diphosphate in this reaction conditions, 7 mM Na_3VO_4 was added to inhibit the phosphatase contamination in the recombinant protein expression and enzyme preparations. Such contamination could potentially result in the degradation of diphosphate group from FPP or GGPP [23]. The outcome of this addition was a 69 % increase in taxadiene production (Fig. S10B).

Moreover, in order to achieve a balanced rate within the system, we tested other seven enzymes to determine their optimal concentration gradients. Results showed that these enzymes could be categorized into three groups based on their effects. Varying the concentration of MVD from 1 to 8 μM did not obviously change the rate of taxadiene synthesis (Fig. 3B and Fig. S11C). The second group, consisting MK, PMK and IDI, showed an increase in taxadiene production from 1.14 to 1.23 folds as their concentrations increased (Fig. S11A, B and D). The third group, the concentrations of GGPPS and tTS remarkably contributed to a 2.08-fold and 1.99-fold increase in taxadiene formation (Figs. S11F and G). Notably, the taxadiene formation decreased with increasing the concentration of $PPK2C^{paN}$ from 1 μM to 5 μM, which was quite likely due to the inhibition effect of high concentration of phosphoric acid on MK and PMK [28] (Fig. S11E). Based on the test of individual enzymes, we slightly adjusted the molar ratio of enzymes MK: PMK: MVD: IDI: PPK: GGPPS: tTS = 15 μM: 15 μM: 1 μM: 15 μM: 1 μM: 60 μM: 80 μM. As a result, the taxadiene production was up to 44.3 mg/L.

To strengthen the synthesis potential of our *in vitro* system, we assayed different concentrations of MVA ranging from 1 to 16 mM. However, there was no significant difference observed in taxadiene output (Fig. S12). We speculated that certain drawbacks needed to be addressed, such as the low activity of TS leading to the accumulation of intermediate GGPP, which in turn had an inhibitory effect on MK (Fig. S13) [28]. To overcome this, we opted a flow addition strategy of MVA and tested various concentrations of GGPPS&tTS to reduce the accumulation of GGPP and enhance downstream reaction rate. The results showed that by adding 2.5 mM MVA, 10 μM GGPPS and 10 μM tTS at each 1 h, the yield of taxadiene to approximately 5-fold, reaching 320.5 mg/L. Moreover, we introduced the enzyme MK from *Methanosarcina mazei,* which has been reported to be resistant to the inhibitory effects of GGPP [28], into the reaction system. Adding 30 μM MmMK in this experiment resulted in a 20 % increase in taxadiene yield (Fig. S14). Subsequently, we enhanced the flux of ATP by reevaluating the loadings of the $PPK2C^{paN}$ and the cofactor PPi. Increasing the amounts of $PPK2C^{paN}$ and PPi to five-fold and two-fold, respectively, led to a 1.7-fold increase in taxadiene production (Fig. 3D and Fig. S15). This result demonstrated that the flux of ATP is highly effective in promoting the reaction of the first three step, thereby impacting the taxadiene formation.

The time gradient of this system was monitored and 547.4 mg/L of taxadiene was produced from total 17.5 mM MVA within 8 h (Fig. 3E), with a conversion rate of ~46.0 % (the molar ratio of MVA to taxadiene is 4:1), which performed below the IUP system (the conversion rate was ~64.7 %) [29]. Besides, our approach requires the integration of more enzymes than the IUP pathway for taxadiene production. Compared to the initial reaction system including six enzymes, $PPK2C^{paN}$ and BST1-ERG20 were both newly introduced into the enzyme cascade reaction. During this optimization process, the types and quantities of enzymes were meticulously adjusted to balance the catalytic rates of the entire pathway. Consequently, identifying the most suitable pH is crucial to maximize the collaborative potential of all enzymes within the modified reaction components [30]. Finally, the findings offered

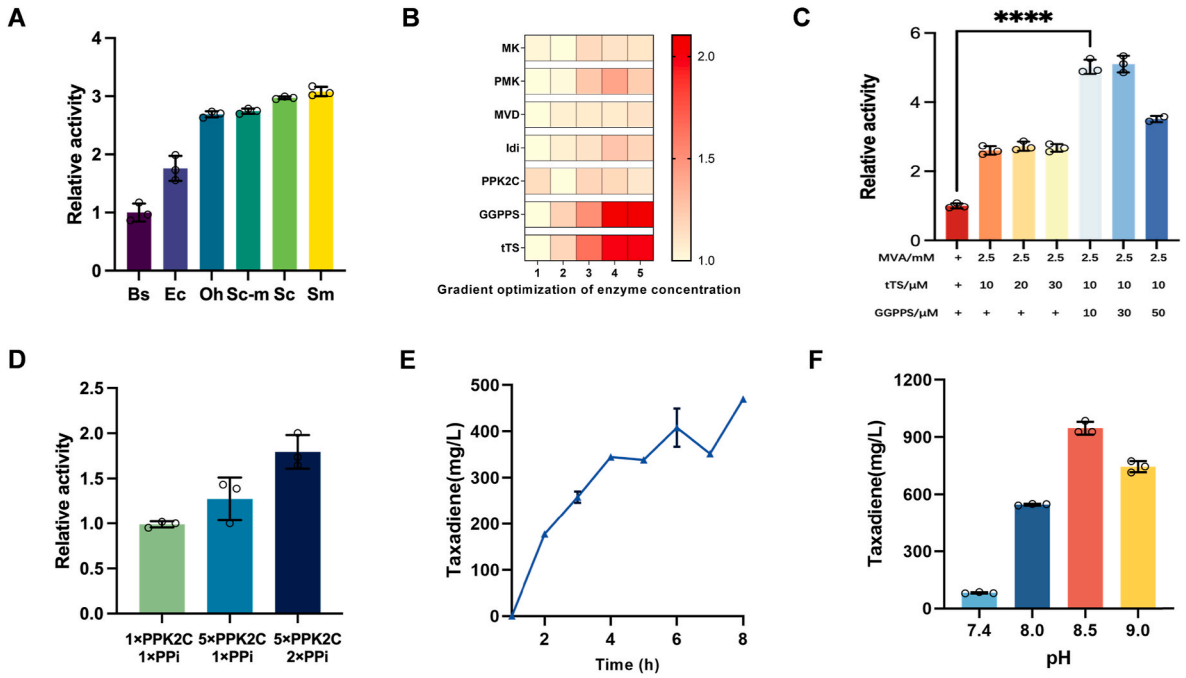

Fig. 3. Improving the yield of taxadiene.
(A) IDI screening. Bs: Idi from *Bacillus subtilis*, Ec: Idi from *E. coli*, OhIdi: Idi from *Oceanihabitans*, Sc-m: Idi from *S. cerevisiae* with Y195F and W256C two mutant sites, Sc: Idi from *S. cerevisiae*, Sm: Idi from *S. miltiorrhiza*. The Y-axis represents the relative yield of taxadiene under different conditions after normalization treatment.
(B) Gradient optimization of the individual enzyme concentrations was conducted with the single variable experiment. The shade of each row represents the relative yield of taxadiene. The horizontal coordinate 1–5 represent the five gradient concentrations of the enzyme and the detail data is described in Supplementary Fig. 9.
(C) The relative activity of taxadiene under different concentrations of MVA, tTS and GGPPS. The red column represents the relative activity of the taxadiene under the 20 mM MVA, 80 μM tTS and 60 μM GGPPS at the beginning of the reaction. The orange, yellow and pale-yellow columns represent the addition of 2.5 mM MVA and 60 μM GGPPS at the beginning of the reaction, titerating the concentration of tTS. The concentration at every hour for tTS or GGPPS was the same as the concentration added at the beginning of the reaction. The Y-axis represents the relative yield of taxadiene under different conditions after normalization treatment.
(D) ATP cycle re-optimization. The Y-axis represents the relative yield of taxadiene under different conditions after normalization treatment.
(E) The yield of taxadiene at different reaction times (2,4,6 and 8 h). The 500 μL reaction system included 50 mM Tris-HCl(pH 8.0), 2.5 mM MVA, 1 mM TCEP, 5 mM ATP,30 mM KCl, 500 mM NaCl, 10 mM $MgCl_2$, 2.4 mM PPi and 7 mM Na_3VO_4.The molar ratio of protein was MmMK: PMK: MVD: SmIDI: $PPK2C^{paN}$: GGPPS: tTS: BST1 - ERG20 = 30 μM: 15 μM: 1 μM: 15 μM: 5 μM: 10 μM: 10 μM: 20 μM. After the initiation of the reaction, 2.5 mM MVA, 10 μM GGPPS, and 10 μM tTS were added hourly until the seventh hour, concluding after a total of 8 h.
(F) The yield of taxadiene at different pH (7.4, 8.0, 8.5 and 9.0). The 500 μL reaction system included 50 mM Tris-HCl at different pH, 2.5 mM MVA, 1 mM TCEP, 5 mM ATP, 30 mM KCl, 500 mM NaCl, 10 mM $MgCl_2$, 2.4 mM PPi and 7 mM Na_3VO_4.The molar ratio of protein was MmMK: PMK: MVD: SmIDI: $PPK2C^{paN}$: GGPPS: tTS: BST1 - ERG20 = 30 μM: 15 μM: 1 μM: 15 μM: 5 μM: 10 μM: 10 μM: 20 μM. After the initiation of the reaction, 2.5 mM MVA, 10 μM GGPPS, and 10 μM tTS were added hourly until the seventh hour, concluding after a total of 8 h.
All data represent the mean of n = 3 biologically independent samples and error bars show standard deviation. The circle represents the raw data.

compelling evidence that a pH value of 8.5 was more favorable for efficient conversion of enzyme cascade reactions, leading to the production of 946.7 mg/L of taxadiene in the ultimately optimized one-pot system (Fig. 3F) and the conversion rate was increased to 79.6 %. Notably, the system at pH 7.4 became turbid when the enzyme mixture was added to the reaction. As the reaction progressed, the white substance was observed to accumulate at the bottom of the reaction system, which indicated that pH 7.4 could not maintain the activity of key enzymes and a small amount of product was formed in the early stage of the reaction.

2.3. Synthesis of taxanes by chemoenzymatic system

The taxadiene produced by the MVA reaction system was extracted by *n*-hexane and purified for subsequent enzyme catalysis or chemical synthesis of T5α-AC. The enzyme reaction system was established as the control by incorporating an N-terminal transmembrane region truncated taxadiene 5-α-hydroxylase (tT5αOH) and a truncated redox partner P450 reductase (tTcCPR). The oxidative products were then subjected to catalysis by TAT. However, only a trace level of acylation product was detected in the T5αOH and TAT system (Fig. S16C). For the chemical synthesis of T5α-AC, palladium-catalyzed acetoxylation of taxadiene was referred to and slightly modified, which is detailed in the supplementary materials [31]. As a result, the C-5α acetoxylation product catalyzed by Pd $(OAc)_2$, benzoquinone, and acetic acid, was obtained as light-yellow viscous liquid at a yield of 48 %. The associated NMR and GC-MS data were consistent with literature reports (Fig. 4B and Figs. S17–19). Introduction of palladium-catalyzed acetoxylation of taxadiene eliminated the need for the inefficient P450 enzyme T5αOH, enabling the synthesis of T5α-AC in available quantities.

Previous studies have speculated that T10βOH is the first post-hydroxylation reaction after acetylation at C5 site. Although T10βOH has been identified for years [32,33], synthesizing C10 oxygenated taxanes in microbial cells is not straightforward due to low catalytic efficiency and precursor deficiencies [34]. Therefore, we plan to construct a cell factory for efficient synthesis of oxygenated taxanes, taking chemically synthesized T5α-Ac as the substrate. *Saccharomyces cerevisiae* is a suitable eukaryotic host with abundant endoplasmic reticulum and better expression capabilities for P450 enzymes. The activities of the T10βOH-1 and T10βOH-2 were initially compared in *S. cerevisiae* W303–1B, and T10βOH-1 was proved to be more active (data not shown), thus it was selected for subsequent chassis construction. Next, the effects of inducible and constitutive promoters on the yield of yeast cells were compared [35]. The inducible promoter

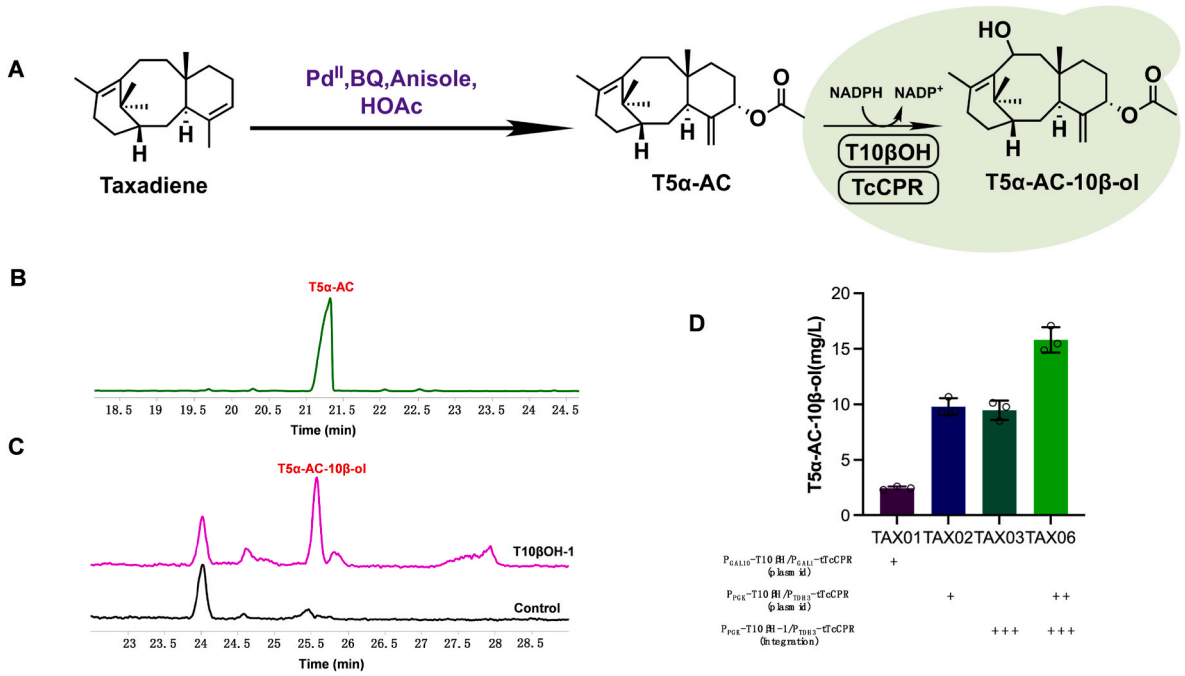

Fig. 4. Chemical and biological coupling for T5α-AC-10β-ol from taxadiene.
(A) The chemical and biological coupling scheme for T5α-AC-10β-ol from taxadiene. Pd^{II}: $Pd(OAc)_2$, BQ: *p*-benzoquinone.
(B) GC analysis of taxadiene C-5α acetoxylation product catalyzed by palladium.Corresponding author:
(C) GC analysis of T10βOH oxidation products of in *S. cerevisiae*.
(D) Comparison of the effects of different promoters and increasing the copy number of T10βOH on T5α-AC-10β-ol yield.
All data represent the mean of n = 3 biologically independent samples and error bars show standard deviation. The circle represents the raw data.

GAL1/GAL10 and strong promoter PGK1/TDH3 were chosen to overexpress T10βOH-1, resulting in strains TAX01 and TAX02 respectively. T5α-AC was used as substrate for TAX01 and TAX02 fermentation, and the fragment peaks of the newly formed product were consistent with those of the reported T5α-AC-10β-ol (*m/z* 346) (Fig. 4C and Fig. S20). Moreover, the output of TAX02 was 3.98 times higher than that of TAX01 (Fig. 4D), leading us to speculate that the constitutive promoter is more suitable for T10βOH-1 expression in this context. Here we observed that there was still substrate residue in the TAX02 fermentation broth. It was speculated that the low catalytic efficiency T10βOH-1 leading to the restricting conversion of substrates because the heterologous expression of plant P450 enzymes was often inefficient. Therefore, we tried to optimize the expression of T10βOH-1 by N-terminal transmembrane engineering and generating fusion protein with truncated TcCPR (tTcCPR) via a short protein linker (GGGGS3). However, these efforts showed no increase in production. To achieve higher yield of T5α-AC-10β-ol, we gradually increased the copy number of T10βOH-1. We constructed a T10βOH-1 multi-copy chassis TAX03 by integrating three copies of T10βOH-1 and tTcCPR into the genome of W303–1B. Then two plasmids carrying T10βOH-1 and tTcCPR were transformed into TAX03 generating TAX06 to further increase the copy number. This led to a 66.7 % increase in the yield of T5α-AC-10β-ol, reaching 15.8 mg/L, which is currently the highest reported yield (Fig. 4D). In conclusion, the above results confirmed that T10βOH-1 and tTcCPR overexpression can effectively convert T5α-AC to T5α-AC-10β-ol. This system can be used for further P450 enzyme functional identification, biosynthesis pathway analysis and heterologous biosynthesis of paclitaxel.

3. Discussion

Although the paclitaxel products market was increased to $1–5 billion per year, the paclitaxel content in Taxus plants was as rare as 0.001%–0.05 % w/w, which is far from enough to meet the market demand [36,37]. The chemical semi-synthesis [38], total chemical synthesis [12] and suspension cell culture have been developed to produce paclitaxel with limited output ratio. At the same time, the catalytic mechanism and process of unknown P450 hydroxylated reactions in the paclitaxel biosynthetic pathway remains unsolved mysteries. Moreover, the high titres of taxane intermediates have been not been achieved to date. Here, our study showed the combination of chemical and biological methods to increase the yield of taxanes intermediates. Within this biochemical hybrid system, we systematically evaluated optimal reaction conditions for biocatalysis across various modules, crucial for maximizing enzyme performance in both the production of taxadiene and T5α-AC-10β-ol. Taxadiene, serving as the core scaffold of taxanes, underwent efficient conversion via tandem enzyme catalysis under one-pot conditions. Notably, the incorporation of a palladium-organometallic catalyst enabled the replacement of the two-step reaction, catalyzed by T5αOH and TAT, with a highly efficient one-step chemical reaction. This innovation uniquely addressed the primary limiting bottleneck posed by T5αOH in the biocatalytic pathway, significantly reducing the formation of oxidative by-products. Moreover, palladium catalysts are often recyclable through appropriate methods, promising reduced system costs and minimized palladium waste. Additionally, we optimized the expression of T10βOH-1 in *S. cerevisiae* to enhance its capacity for utilizing T5α-AC as a substrate. Compared to the biosynthesis pathway from xylose to T5α-AC-10β-ol [39], the total yield of this efficient chemo-enzyme hybrid system was elevated for more than 2000-fold (Fig. S21).

Establishing a concise *in vitro* reaction system is conducive to be more flexible controlled than the complex cellular metabolism, and can be expediently optimized at different levels. In this study, the taxadiene module was mainly optimized at three different level, including the cofactor optimization, enzyme component optimization, and pathway upstream and downstream optimization. Compared to the IUP pathway, we introduced PPK for the ATP regeneration. However, the addition of polyphosphoric acid donor will lead to the accumulation of phosphoric

acid ions, which have a detrimental effect on the enzyme-element. And the damage is aggravated due to the hydrolysis of intermediates GGPP and the formation of byproduct PPi catalyzed by GGPPS. We replaced the ATP regeneration system of $PPK2C^{paN}$ to reduce the inhibition of the accumulation of phosphate ion on enzyme activity. Moreover, a fusion protein BST1-ERG20 was added to increase the GGPP flux and 7 mM Na_3VO_4 was added to inhibit the hydrolysis of GGPP phosphate group. The system is robust for the production of taxadiene and the productivity operates 14.2-fold higher than microbial fermentation. The optimized information of enzyme quantity and cofactors acquired in this *in vitro* system also guided the rationally modifying of the engineered microbes to produce taxadiene derivates.

In the future work, the reaction conditions could be further optimized and the T10βOH reaction can be attempted in a superior host or mutation. In addition, although we circumvented the T5αOH catalysis problem here and achieved the synthesis of the intermediates with relative high yield, we speculated that other enzymes might catalyze the oxidation reaction at C5 in the process of paclitaxel synthesis needs to be further discovered. Although the minimal gene set was been successfully tested, elucidating the complete biosynthetic mechanism and reaction order of paclitaxel and achieving industrial-scale production of paclitaxel with synthetic biology still requires extensive efforts. Initiating mass synthesis of taxadiene, T5α-AC and T5α-AC-10β-ol with biochemical coupling methods conducted in this study as a promising step to accelerate subsequent catalytic reactions and accelerate the biosynthesis process of paclitaxel and its derivatives.

In summary, this study achieves synergistic integration of biocatalysis with chemical synthesis, achieving complementary advantages and providing a concise and efficient synthetic model for the artificial synthesis of complex plant natural products. The bio-chemical coupling synthesis method will not only provide profound changes in pharmaceutical industry, but also expand the scientific foundation of synthetic biology and facilitates interdisciplinary integration.

4. Methods

4.1. Plasmid construction

All methods in this article are detailed in Supplementary Information, including plasmid construction; expression and purification of enzymes; synthesis of taxadiene from MVA *in vitro*; IDI screening; enzymatic reaction assay for T5α-AC from taxadiene; chemical synthesis of T5α-AC; overexpression of taxane 10β-hydroxylase in *S. cerevisiae* and GC-MS analysis of the target compounds.

4.2. Statistics and reproducibility

All experimental data were at least in triplicate and expressed as means ± standard errors. All data analysis was performed by Excel or GraphPad Prism.

4.3. Data, materials, and software availability

The data reported in this article are available in the main text or the Supplementary Information.

Declaration of competing interest

The authors declare no competing financial interest.

CRediT authorship contribution statement

Jing Li: designed and wrote the paper and conducted relevant experiments. **Xiaonan Liu:** designed and wrote the paper and conducted relevant experiments, revised the paper. **Xiaoxi Zhu:** designed and wrote the paper and conducted relevant experiments. **Jiayu Liu:** conducted relevant experiments. **Lei Zhang:** conducted relevant experiments. **Nida Ahmed:** revised the paper. **Jian Qi:** conducted relevant experiments. **Bihuan Chen:** conducted relevant experiments. **Daliang Tang:** Chemical synthesis of T5α-AC. **Jinsheng Yu:** Chemical synthesis of T5α-AC. **Zhijin Fan:** revised the manuscript. **Huifeng Jiang:** revised the manuscript.

Acknowledgements

This work was supported in part by the National Natural Science Foundation of China (32371499, 31901026 and 32172443), China Postdoctoral Science Foundation (2019M661032); National Key R&D Program of China (2020YFA0908000 and 2022YFD1700400); the Frontiers Science Center for New Organic Matter, Nankai University (63181206) and the Tianjin Development Program for Innovation and Entrepreneurship (2019-06).

Appendix A. Supplementary data

Supplementary data to this article can be found online at https://doi.org/10.1016/j.synbio.2024.05.002.

References

[1] Mutanda I, Li J, Xu F, Wang Y. Recent advances in metabolic engineering, protein engineering, and transcriptome-guided insights toward synthetic production of taxol. Front Bioeng Biotechnol 2021;9:632269.
[2] Tong Y, Luo YF, Gao W. Biosynthesis of paclitaxel using synthetic biology. Phytochemistry Rev 2021;21(3):863–77.
[3] Zhang Y, Wiese L, Fang H, Alseekh S, Perez de Souza L, Scossa F, Molloy J, Christmann M, Fernie AR. Synthetic biology identifies the minimal gene set required for Paclitaxel biosynthesis in a plant chassis. Mol Plant 2023;16(12):1951–61.
[4] Jiang B, Gao L, Wang H, Sun Y, Zhang X, Ke H, Liu S, Ma P, Liao Q, Wang Y, Wang H, Liu Y, Du R, Rogge T, Li W, Shang Y, Houk KN, Xiong X, Xie D, Huang S, Lei X, Yan J. Characterization and heterologous reconstitution of Taxus biosynthetic enzymes leading to baccatin III. Science 2024;383(6683):622–9.
[5] Yang C, Wang Y, Su Z, Xiong L, Wang P, Lei W, Yan X, Ma D, Zhao G, Zhou Z. Biosynthesis of the highly oxygenated tetracyclic core skeleton of Taxol. Nat Commun 2024;15(1):2339.
[6] Chun-Ting Liu J, De La Pena R, Tocol C, Sattely ES. Reconstitution of early paclitaxel biosynthetic network. Nat Commun 2024;15(1):1419.
[7] Edgar S, Zhou K, Qiao K, King JR, Simpson JH, Stephanopoulos G. Mechanistic insights into taxadiene epoxidation by taxadiene-5alpha-hydroxylase. ACS Chem Biol 2016;11(2):460–9.
[8] Edgar S, Li FS, Qiao K, Weng JK, Stephanopoulos G. Engineering of taxadiene synthase for improved selectivity and yield of a key taxol biosynthetic intermediate. ACS Synth Biol 2017;6(2):201–5.
[9] Song X, Wang Q, Zhu X, Fang W, Liu X, Shi C, Chang Z, Jiang H, Wang B. Unraveling the catalytic mechanism of taxadiene-5α-hydroxylase from crystallography and computational analyses. ACS Catal 2024:3912–25.
[10] Nowrouzi B, Lungang L, Rios-Solis L. Exploring optimal Taxol(R) CYP725A4 activity in Saccharomyces cerevisiae. Microb Cell Factories 2022;21(1):197.
[11] Walls LE, Malci K, Nowrouzi B, Li RA, d'Espaux L, Wong J, Dennis JA, Semiao AJC, Wallace S, Martinez JL, Keasling JD, Rios-Solis L. Optimizing the biosynthesis of oxygenated and acetylated Taxol precursors in Saccharomyces cerevisiae using advanced bioprocessing strategies. Biotechnol Bioeng 2021;118(1):279–93.
[12] Min L, Han J-C, Zhang W, Gu C-C, Zou Y-P, Li C-C. Strategies and lessons learned from total synthesis of taxol. Chem Rev 2023;123(8):4934–71.
[13] Hu Y-J, Gu C-C, Wang X-F, Min L, Li C-C. Asymmetric total synthesis of taxol. J Am Chem Soc 2021;143(42):17862–70.
[14] Chen X, Zhang C, Zou R, Stephanopoulos G, Too HP. In vitro metabolic engineering of amorpha-4,11-diene biosynthesis at enhanced rate and specific yield of production. ACS Synth Biol 2017;6(9):1691–700.
[15] Zhu F, Zhong X, Hu M, Lu L, Deng Z, Liu T. In vitro reconstitution of mevalonate pathway and targeted engineering of farnesene overproduction in Escherichia coli. Biotechnol Bioeng 2014;111(7):1396–405.
[16] Korman TP, Opgenorth PH, Bowie JU. A synthetic biochemistry platform for cell free production of monoterpenes from glucose. Nat Commun 2017;8:15526.
[17] Ward VCA, Chatzivasileiou AO, Stephanopoulos G. Cell free biosynthesis of isoprenoids from isopentenol. Biotechnol Bioeng 2019;116(12):3269–81.
[18] St Paul M, Saibil SD, Han S, Israni-Winger K, Lien SC, Laister RC, Sayad A, Penny S, Amaria RN, Haydu LE, Garcia-Batres CR, Kates M, Mulder DT, Robert-Tissot C, Gold MJ, Tran CW, Elford AR, Nguyen LT, Pugh TJ, Pinto DM, Wargo JA, Ohashi PS. Coenzyme A fuels T cell anti-tumor immunity. Cell Metabol 2021;33(12):2415–2427.e6.
[19] Li Y-H, Xia Y, Zhang Z, Wang B, Jin R-J, Chen C-H, Chen J, Wang K-L, Xing G, Wang Z-K, Liao L-S. In situ hydrolysis of phosphate enabling sky-blue perovskite light-emitting diode with EQE approaching 16.32. ACS Nano 2024;18(8):6513–22.

[20] Liyang Y, Qiang G, Jifang L, Bangyuan Z, Guilan L, JianQuan G. Opportunities and challenges of in vitro synthetic biosystem for terpenoids production. Biotechnol Bioproc Eng 2022;27:697–705.
[21] Andexer JN, Richter M. Emerging enzymes for ATP regeneration in biocatalytic processes. Chembiochem 2015;16(3):380–6.
[22] Ajikumar Parayil Kumaran XW-H, Tyo Keith EJ, Wang Yong, Fritz Simeon, Effendi Leonard, Effendi Mucha, Too Heng Phon, Blaine Pfeifer. Stephanopoulos gregory isoprenoid pathway optimizationfor taxol precursor OverproductioninEscherichia coli. Science 2010;330(6000):4.
[23] Dirkmann M, Nowack J, Schulz F. An in vitro biosynthesis of sesquiterpenes starting from acetic acid. Chembiochem 2018;19(20):2146–51.
[24] Chen X, Zhang C, Zou R, Zhou K, Stephanopoulos G, Too HP. Statistical experimental design guided optimization of a one-pot biphasic multienzyme total synthesis of amorpha-4,11-diene. PLoS One 2013;8(11):e79650.
[25] Dong C, Qu G, Guo J, Wei F, Gao S, Sun Z, Jin L, Sun X, Rochaix J-D, Miao Y, Wang R. Rational design of geranylgeranyl diphosphate synthase enhances carotenoid production and improves photosynthetic efficiency in Nicotiana tabacum. Sci Bull 2022;67(3):315–27.
[26] Zhou YJ, Gao W, Rong Q, Jin G, Chu H, Liu W, Yang W, Zhu Z, Li G, Zhu G, Huang L, Zhao ZK. Modular pathway engineering of diterpenoid synthases and the mevalonic acid pathway for miltiradiene production. J Am Chem Soc 2012;134(6):3234–41.
[27] Hu T, Zhou J, Tong Y, Su P, Li X, Liu Y, Liu N, Wu X, Zhang Y, Wang J, Gao L, Tu L, Lu Y, Jiang Z, Zhou YJ, Gao W, Huang L. Engineering chimeric diterpene synthases and isoprenoid biosynthetic pathways enables high-level production of miltiradiene in yeast. Metab Eng 2020;60:87–96.
[28] Primak YA, Du M, Miller MC, Wells DH, Nielsen AT, Weyler W, Beck ZQ. Characterization of a feedback-resistant mevalonate kinase from the archaeon Methanosarcina mazei. Appl Environ Microbiol 2011;77(21):7772–8.
[29] Chatzivasileiou AO, Ward V, Edgar SM, Stephanopoulos G. Two-step pathway for isoprenoid synthesis. Proc Natl Acad Sci USA 2019;116(2):506–11.
[30] Tang S, Chen Y, Liao D, Lin Y, Han S, Zheng S. A process for p-hydroxystyrene production from glycerol based on cell-free biosynthesis system. Biochem Eng J 2023;195:108927.
[31] Wilde NC, Isomura M, Mendoza A, Baran PS. Two-phase synthesis of (-)-taxuyunnanine D. J Am Chem Soc 2014;136(13):4909–12.
[32] Guo B, Kai G, Gong Y, Jin H, Wang Y, Miao Z, Sun X, Tang K. Molecular cloning and heterologous expression of a 10-deacetylbaccatin III-10-O-acetyl transferase cDNA from Taxus x media. Mol Biol Rep 2007;34(2):89–95.
[33] Jennewein S, Long RM, Williams RM, Croteau R. Cytochrome p450 taxadiene 5alpha-hydroxylase, a mechanistically unusual monooxygenase catalyzing the first oxygenation step of taxol biosynthesis. Chem Biol 2004;11(3):379–87.
[34] Dejong JM, Liu Y, Bollon AP, Long RM, Jennewein S, Williams D, Croteau RB. Genetic engineering of taxol biosynthetic genes in Saccharomyces cerevisiae. Biotechnol Bioeng 2006;93(2):212–24.
[35] Liu X, Cheng J, Zhang G, Ding W, Duan L, Yang J, Kui L, Cheng X, Ruan J, Fan W, Chen J, Long G, Zhao Y, Cai J, Wang W, Ma Y, Dong Y, Yang S, Jiang H. Engineering yeast for the production of breviscapine by genomic analysis and synthetic biology approaches. Nat Commun 2018;9(1):448.
[36] Cheng J, Wang X, Liu X, Zhu X, Li Z, Chu H, Wang Q, Lou Q, Cai B, Yang Y, Lu X, Peng K, Liu D, Liu Y, Lu L, Liu H, Yang T, Ge Q, Shi C, Liu G, Dong Z, Xu X, Wang W, Jiang H, Ma Y. Chromosome-level genome of Himalayan yew provides insights into the origin and evolution of the paclitaxel biosynthetic pathway. Mol Plant 2021;14(7):1199–209.
[37] Zhang Y, Wiese L, Fang H, Alseekh S, Perez de Souza L, Scossa F, Molloy J, Christmann M, Fernie AR. Synthetic biology identifies the minimal gene set required for Paclitaxel biosynthesis in a plant chassis. Mol Plant 2023;16(12):1951–61.
[38] Jennewein S, Croteau R. Taxol: biosynthesis, molecular genetics, and biotechnological applications. Appl Microbiol Biotechnol 2001;57(1–2):13–9.
[39] Zhou K, Qiao K, Edgar S, Stephanopoulos G. Distributing a metabolic pathway among a microbial consortium enhances production of natural products. Nat Biotechnol 2015;33(4):377–83.